

Recovery of the Rod Photoresponse in Infants

Ronald M. Hansen and Anne B. Fulton

PURPOSE. To study deactivation of the rod photoresponse in infants using a paired-flash procedure. Rhodopsin content increases and scales the parameters of the activation of rod phototransduction as rods develop. However, little is known about the kinetics of deactivation in the rods of young infants.

METHODS. ERG responses to pairs of flashes were used to study the recovery of the rod response in 4- and 10-week-old infants and mature control subjects. The amplitudes of rod isolated a-wave responses to a probe flash ($+3.3 \log \text{scot td} \cdot \text{s}$) presented 2 to 120 seconds after an equal-intensity test flash were measured. The interstimulus interval (ISI) at which the amplitude was half that of the response to the probe flash alone (t_{50}) was determined by linear interpolation.

RESULTS. Recovery time (t_{50}) was significantly longer in infants than in adults ($F = 18.9$, $df 2, 32$; $P < 0.01$). The shape of the recovery function did not vary with age. The t_{50} values were inversely proportional to the parameters of activation of rod phototransduction.

CONCLUSIONS. These results are evidence that the kinetics of deactivation in infants are slower and may be set by the proportion of rhodopsin isomerized. (*Invest Ophthalmol Vis Sci*. 2005;46:764-768) DOI:10.1167/iovs.04-0257

As postnatal development of the retina proceeds, rod outer segments elongate, and the rhodopsin content of the retina increases.¹⁻³ During development, rhodopsin content scales the parameters of the activation of phototransduction in the dark-adapted eye.⁴⁻⁷

Less is known about deactivation—that is, recovery—of the immature rod photoresponse. In a series of molecular events, the rod photoresponse recovers by stepwise deactivation of rhodopsin, transducin, and phosphodiesterase.⁸⁻¹¹ With the developmental elongation of the rod outer segments, several of the proteins involved in the recovery of the rod response have been shown to increase.¹²⁻¹⁶ In infant rat rods, the kinetics of the recovery of the photoresponse appear to be slower than in adults and to be governed by the proportion of rhodopsin isomerized/rod/flash.¹⁷

We used a paired-flash ERG procedure to study recovery of the rod photoresponse in 4- and 10-week-old infants and adult control subjects. Double-flash procedures have permitted successful summarization of the kinetics of rod cell recovery in healthy adults, patients, and animals, including immature rats.^{10,17-20} We tested the hypothesis that t_{50} , the time at which the rod response had recovered to half its dark-adapted amplitude, differed significantly between infants and adults.

From the Department of Ophthalmology, Children's Hospital and Harvard Medical School, Boston, Massachusetts.

Supported by National Eye Institute Grant EY10597.

Submitted for publication March 5, 2004; revised June 9 and September 27, 2004; accepted October 24, 2004.

Disclosure: **R.M. Hansen**, None; **A.B. Fulton**, None

The publication costs of this article were defrayed in part by page charge payment. This article must therefore be marked "advertisement" in accordance with 18 U.S.C. §1734 solely to indicate this fact.

Corresponding author: Ronald M. Hansen, Department of Ophthalmology, Children's Hospital and Harvard Medical School, 300 Longwood Avenue, Boston, MA 02115; ronald.hansen@childrens.harvard.edu.

METHODS

ERG responses were recorded by using previously reported procedures.⁶ The pupils were dilated with cyclopentolate hydrochloride 1%, and the subjects were dark adapted for 30 minutes. Then, in dim red light, proparacaine hydrochloride 0.5% was instilled, and a Burian-Allen bipolar electrode (Hansen Ophthalmic Development Laboratories, Solon, IA) was placed on the left eye. A ground electrode was placed on the skin over the left mastoid.

Brief ($<1 \text{ ms}$), blue (Wratten 47B, $\lambda < 510 \text{ nm}$; Eastman Kodak Co., Rochester, NY) stimuli (model 600VR, series 2100; Novatron, Dallas, TX) were delivered through a 41-cm integrating sphere, controlled in intensity by calibrated, neutral-density filters and ranged from those evoking a small ($<15 \mu\text{V}$) b-wave to those that saturated the a-wave amplitude in normal subjects.⁶ Responses were differentially amplified (AC-coupled 1-1000 Hz; 1000 gain), displayed on an oscilloscope, and stored on a disk for analysis later (Compact 4; Nicolet Biomedical Instruments, Madison, WI).⁶

The unattenuated flash was measured with a detector (model S350; United Detector Technology, Orlando, FL) placed at the position of the subject's cornea. This produced approximately $3.3 \log \text{scot td} \cdot \text{s}$. The retinal illuminance produced by the stimulus varies directly with pupil diameter and transmissivity of the ocular media and inversely with the square of the posterior nodal distance of the eye.²¹ We used direct measurement of the dilated pupils of our subjects and measurements of the ocular media density^{22,23} and ocular dimensions²⁴ to calculate retinal illuminance. Equal-intensity stimuli produce approximately equal retinal illuminances for both infants and adults.²⁵⁻²⁷

Activation of Phototransduction in Rods

The parameters of the activation of the rod photoresponse were estimated using the Hood and Birch²⁸ modification of the Lamb and Pugh^{4,5} model of the biochemical processes involved in the activation of rod phototransduction. A curve-fitting routine (MatLab, fmins; The MathWorks, Natick, MA) was used to determine the best-fitting values of S ($\text{scot td}^{-1} \cdot \text{s}^{-3}$), $R_{\text{mp}3}$ (in microvolts) and t_d (in seconds) in the equation

$$R(I, t) = \{1 - \exp[-0.5 IS(t - t_d)^2]\} R_{\text{mp}3}. \quad (1)$$

Fitting of the model was restricted to the leading edge of the a-wave response or to a maximum of 20 ms after stimulus onset. I is the scotopic troland value of the stimulus, and t_d is a brief delay.

Estimation of Isomerizations Produced by the Stimuli

To estimate the number of isomerizations (ϕ) produced by the stimuli, we followed previously described methods²⁹⁻³¹ and used the equation

$$\theta = L \cdot A \cdot t(\lambda) k(\lambda) (1 - 10^{-D_\lambda}) \gamma. \quad (2)$$

In this equation, L is the luminance of the stimulus (in candelas per square meter), A is the area of the pupil, and $t(\lambda)$ the transmissivity of the ocular media. The constant $k(\lambda)$ includes the posterior nodal distance, the scotopic luminance efficiency (V'_λ), the end-on collecting area of a single rod, and the wavelength of the stimulus (λ). The quantum efficiency of isomerization (γ) and the optical density of rhodopsin (D_λ) are the other terms in the equation. For the conversion,

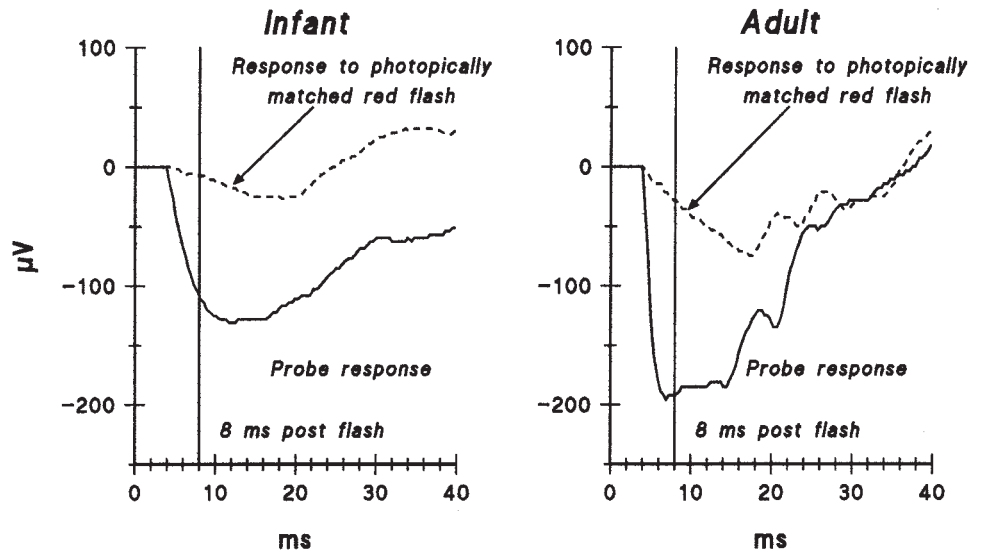


FIGURE 1. Rod isolation. Sample responses in a 4-week-old infant and an adult are shown. The amplitude of the a-wave response to a photopically matched red flash (*dashed trace*) was subtracted from the a-wave response to the probe flash. The amplitude of the rod isolated a-wave measured 8 ms after the flash was used in the analyses.

the end-on collecting area of the rod and quantum efficiency of isomerization are assumed to be the same in infants and adults. Further, the axial density of rhodopsin in the outer segment is taken to be proportional to the rhodopsin content of the retina,³ and thus, the ratio of infant to adult isomerizations is proportional to $(1-10^{-D_{\text{infant}}})/(1-10^{-D_{\text{adult}}})$.

From the human rhodopsin growth curve,³ 4-week-old infants have 46% and 10-week-olds 68% of the adult rhodopsin density of 0.4. Therefore, optical density is 0.18 at 4 weeks and 0.27 at 10 weeks, and the calculated ratio of $(1-10^{-D_{\text{infant}}})/(1-10^{-D_{\text{adult}}})$ is 0.56 at 4 weeks and 0.77 at 10 weeks. Thus, 1 scot $\text{td} \cdot \text{s}$ isomerizes 4.8 molecules of rhodopsin in 4-week-olds, 6.6 molecules in 10-week-olds, and 8.5 molecules in adults.

The main parameters of the model are S and $R_{\text{mp}3}$. S is a sensitivity parameter related to the gain of activation. It is based on the time constants of the molecular processes involved in the activation of phototransduction.^{4,5} The saturated amplitude of the response, $R_{\text{mp}3}$, represents the number of channels in the outer segment membrane that are available for closure by light.^{4,5} In immature rat and human retina, both S and $R_{\text{mp}3}$ are proportional to the rhodopsin content of the retina.^{3,6,7}

Deactivation of Phototransduction in Rods

The recovery of the rod cell's response to light was evaluated with a paired-flash paradigm.¹⁹ At seven selected interstimulus intervals (ISIs) after the test flash (2–120 seconds), a probe flash was presented. The probe and test flashes were of equal intensity and were estimated to produce $+3.3 \log \text{scot td} \cdot \text{s}$. Between each test-probe pair, 2 minutes in the dark was allowed. Control experiments in adults and preliminary observations in infants showed that 2 minutes were sufficient for full recovery to the amplitude of the dark-adapted response. The amplitude of the a-wave response to a photopically matched red ($\lambda > 600 \text{ nm}$) flash was subtracted from the response to the probe flash.³² The amplitude of the a-wave was measured 8 ms after the flash to minimize contamination by postreceptor components (Fig. 1). The amplitude of R , the rod-isolated a-wave response to the probe was expressed as the proportion of amplitude of the a-wave response to the probe flash alone, R_{max} . The response to the probe flash provides a measure of the circulating current in the rods.^{18,19,33} Linear interpolation was used to determine the time, t_{50} , at which a-wave amplitude was half the maximum a-wave amplitude. Thus, recovery was characterized without making assumptions about the shape of the recovery function.¹⁹

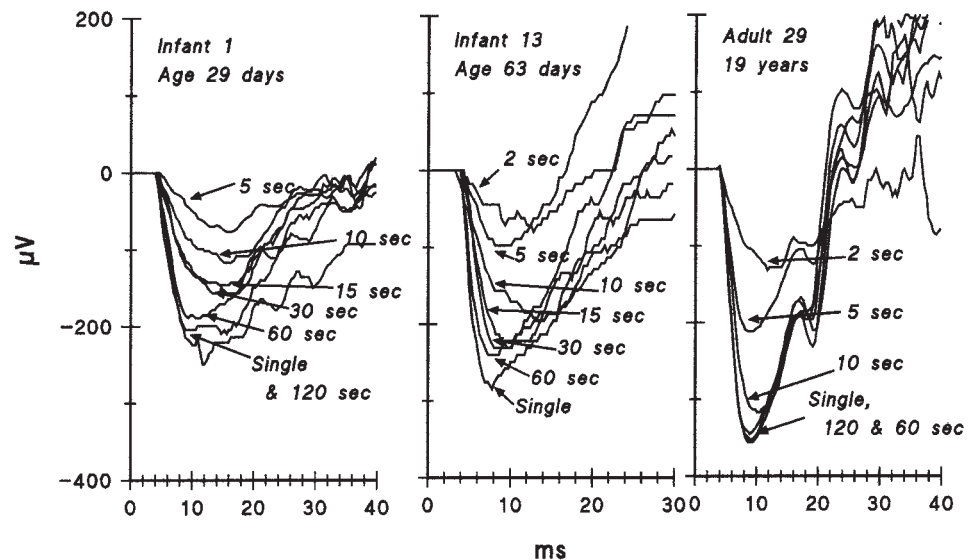


FIGURE 2. Sample a-wave responses from a 29-day-old infant (*left*), a 63-day-old infant (*middle*), and a 19-year-old control subject (*right*). The ISI is indicated.

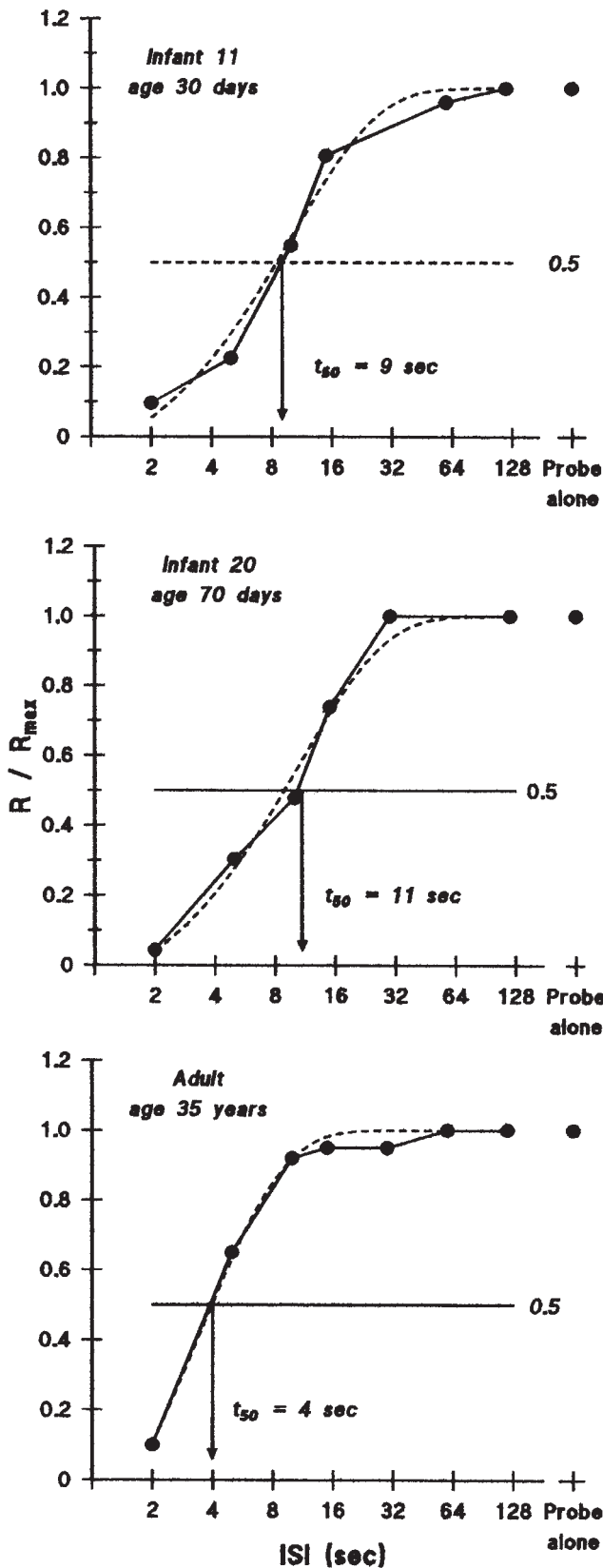


FIGURE 3. For the rod-isolated response, a-wave amplitude measured 8 ms after the flash expressed as a fraction of R_{max} is plotted as a function of ISI for a representative subject from each age group. The ISI that would produce a half-maximum response was determined by linear interpolation and is indicated by the arrows. These subjects had t_{50} close to the median for their ages. The smooth curves represent equation 2 fit to the data.

To determine whether the shape of the R/R_{max} versus ISI function varies with age, the equation

$$R/R_{max} = 1 - \exp[-(t - T_c)/\tau] \tag{3}$$

was fit to each subject's data. T_c is the delay (in seconds) before the start of recovery, and τ is the time constant (in seconds) of the exponential function.^{18,19} In fitting equation 3, T_c was constrained to be ≥ 0 .

Subjects

Infants, aged 4 weeks (23–39 days; median, 31 days; $n = 12$) and 10 weeks (63–77 days; median, 70 days; $n = 15$) were recruited by mail. All subjects were born within 10 days of term. The median age of mature control subjects was 22 years (8–40 years; $n = 8$). Thorough ophthalmic examination showed all had normal eyes. The study was reviewed and approved by the Children's Hospital Committee on Clinical Investigation and adhered to the tenets of the Declaration of Helsinki. Written, informed consent was obtained from the parents and control subjects before testing. The activation parameters (S and R_{mp3}) of all subjects have been included in a previous report.⁶ In our laboratory, the values of S in the mature control subjects are higher than those reported by others.³⁴ Recovery data from the control subjects have been reported.³⁵

RESULTS

For records such as those in Figure 2, a-wave amplitude was measured at 8 ms after the stimulus. Rod-isolated a-wave amplitude was expressed as a proportion of the a-wave response to the probe presented alone (R/R_{max}) and plotted as a function of ISI (Fig. 3). The parameters of the exponential recovery function are summarized in Table 1. The fit of equation 2 to such functions was reasonable at all ages (Table 1). The time constant (τ) of this function varied significantly with age (ANOVA; $F = 8.3$; $df\ 2, 32$; $P < 0.01$), but the delay in recovery (T_c) did not (ANOVA; $F = 0.23$; $df\ 2, 32$; NS).

Recovery time (t_{50}), determined by linear interpolation (Fig. 4), decreased significantly with age (ANOVA; $F = 18.9$; $df\ 2, 32$; $P < 0.01$). The average t_{50} (\pm SEM) was 9.7 ± 0.7 seconds in the 4-week-olds, 10.6 ± 0.8 seconds in the 10-week-olds, and 4.5 ± 0.3 seconds in the adults. Friedburg et al.³³ used equal-intensity test and probe flashes (8,200 or 11,000 scot td · s) with two adults; the rod isolated t_{50} , determined by linear interpolation, was 5 and 3.5 seconds, respectively.

The median values of t_{50} were the same at ages 4 and 10 weeks. Post hoc analysis (Scheffé test) showed that while t_{50} at 4 and 10 weeks differed significantly ($P < 0.05$) from that of control subjects, the infant t_{50} did not differ significantly between 4 and 10 weeks. There was good agreement between recovery time (t_{50}) estimated by linear interpolation and τ calculated by using equation 3. Recovery time t_{50} correlated with the time constant of the exponential function τ ($r = 0.84$; $df\ 33$; $P < 0.01$). In contrast to the results herein, Pepperberg et al.³² found that the recovery time in a single 6-week-old infant was the same as in adults. In that study,³² the test flash

TABLE 1. Summary of Deactivation Results

Age	t_{50} (s)	τ (s)	T_c (s)	r^2
4 weeks	9.7 (0.7)	11.0 (1.1)	1.7 (0.1)	0.96 (0.01)
10 weeks	10.6 (0.8)	10.7 (1.1)	1.9 (0.2)	0.93 (0.01)
Adult	4.5 (0.3)	4.8 (0.5)	1.8 (0.1)	0.97 (0.01)

The proportion of variance accounted for by equation 3 is indexed by r^2 . Data are the mean \pm (SEM).

was 200 to 300 scot td · s, and the probe flash was 10,000 scot td · s, whereas in the present study both the test and probe flashes were 2,000 scot td · s.

There were significant correlations between S , the activation parameter, and t_{50} , the deactivation parameter (Fig. 5, top). Higher S was associated with shorter t_{50} ($r = -0.61$; df 33; $P < 0.01$). S , expressed in the number of molecules of rhodopsin isomerized by the stimuli, also correlated significantly with t_{50} ($r = -0.64$; df 33; $P < 0.01$). In addition, saturated amplitude of the rod response (Fig. 5, bottom), R_{mp3} , was inversely related to t_{50} ($r = -0.59$; df 33; $P < 0.01$).

DISCUSSION

Deactivation of the rod photoresponse in infants appears slower than in adults. In infants the recovery time, t_{50} , is significantly longer than in adults (Fig. 4). The overlap in t_{50} and also S and R_{mp3} in 4- and 10-week-old infants may in part be due to variability inherent in the ERG parameters and to the small difference in average rhodopsin content (46% vs. 68%) at these ages.³

In adults, the kinetics of recovery depend on the intensity of the test flash.¹⁸ Prolonged recovery is associated with brighter test flashes and shorter recovery times with less intense test flashes. Variation in probe flash intensity has little effect on recovery time.³³ Thus, the present results obtained with a 2000-scot td · s test flash (Fig. 4) together with those in the 2-month-old infant studied with a 200-scot td · s test flash are consistent with the relationship of test flash intensity and recovery time differing between infants and adults. These results in infants are in accord with the results obtained in immature rat rods that were studied with a range of test flash intensities.¹⁷

The recovery time, t_{50} , correlated inversely (Fig. 5) with the parameters of activation of the rod response, S and R_{mp3} , both of which are scaled by rhodopsin content of the retina during development.^{6,7} Thus, rhodopsin content appears to be an important determinant of the parameters of both activation and deactivation in the immature retina.

Possibly, the kinetics of recovery are set by the probability of encounters of activated rhodopsin, R^* , with the proteins

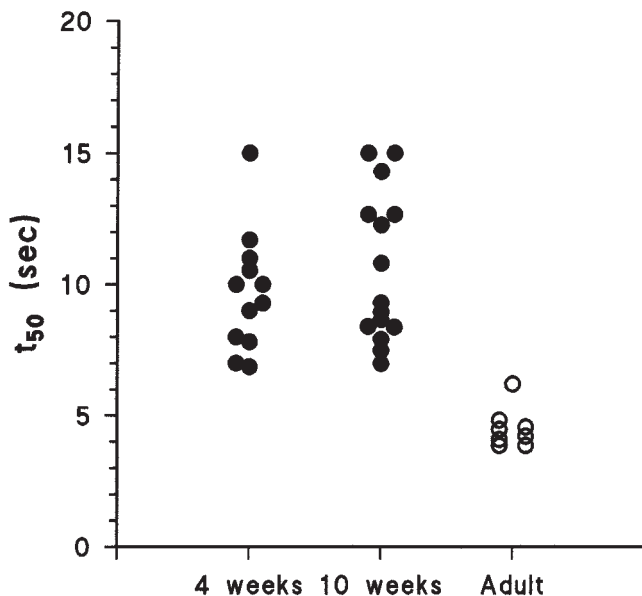


FIGURE 4. Individual t_{50} s determined by linear interpolation are plotted for the three age groups.

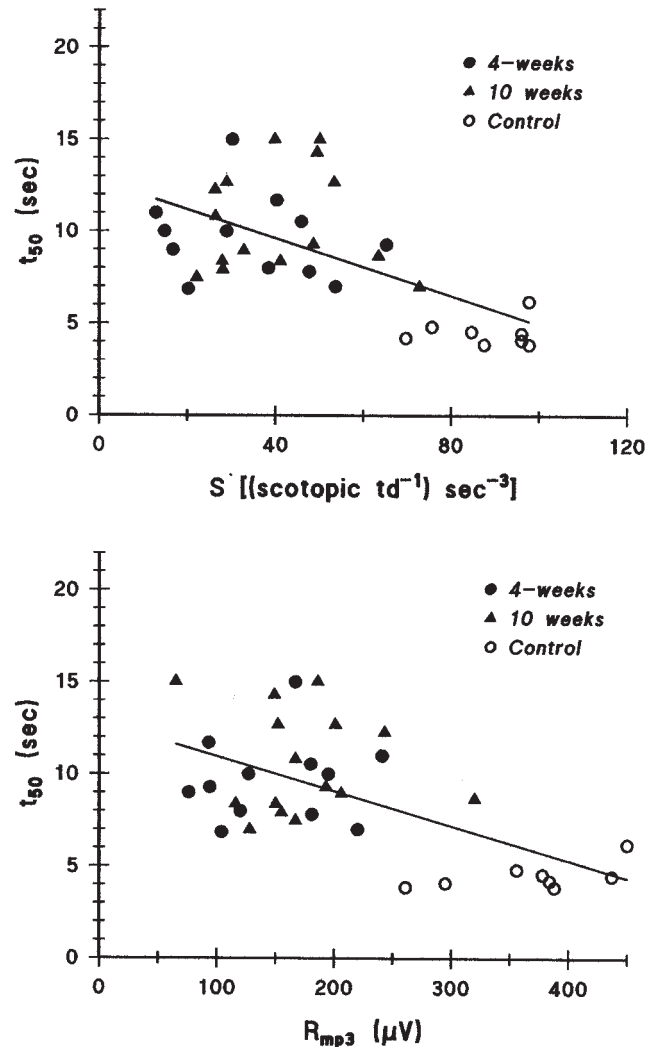


FIGURE 5. Top: the parameter t_{50} is plotted as a function of S , the parameter that reflects the gain of the steps involved in the activation of phototransduction. Bottom: the deactivation parameter t_{50} is plotted as a function of R_{mp3} , the parameter that reflects the number of channels available for closure by light.

involved in deactivation.^{10,19} Another explanation for prolonged recovery in infants is the possibility that the concentration of one or more of the proteins involved in deactivation differs between infants and adults. However, at present we know of no evidence that the concentration of any of the proteins involved in deactivation is low in the immature rod,¹²⁻¹⁶ although, admittedly, the development of each protein has yet to be studied.

Acknowledgments

The authors thank Baharek Asefzadah, Marta Jolesz, Annie Gee, and Nicole Couture for their assistance.

References

- Hendrickson AE. The morphologic development of human and monkey retina. In: Albert DM, Jakobiec FA, eds. *Principles and Practice of Ophthalmology: Basic Sciences*. Philadelphia: WB Saunders Co.; 1994:561-577.
- Hendrickson AE, Drucker D. The development of parafoveal and midperipheral retina. *Behav Brain Res*. 1992;19:21-32.

3. Fulton AB, Dodge J, Hansen RM, Williams TP. The rhodopsin content of human eyes. *Invest Ophthalmol Vis Sci.* 1999;40:1878-1883.
4. Lamb TD, Pugh EN Jr. A quantitative account of the activation steps involved in phototransduction in amphibian photoreceptors. *J Physiol (Lond).* 1992;449:719-758.
5. Pugh EN Jr, Lamb TD. Amplification and kinetics of the activation steps in phototransduction. *Biochem Biophys Acta.* 1993;1141:111-149.
6. Fulton AB, Hansen RM. The development of scotopic sensitivity. *Invest Ophthalmol Vis Sci.* 2000;41:1588-1596.
7. Fulton AB, Hansen RM, Findl O. The development of the rod photoresponse from dark-adapted rats. *Invest Ophthalmol Vis Sci.* 1995;36:1038-1045.
8. Arshavsky VY. Rhodopsin phosphorylation: from terminating single photon responses to photoreceptor dark adaptation. *Trends Neurosci.* 2002;25:124-126.
9. Burns ME, Baylor DA. Activation, deactivation, and adaptation in vertebrate photoreceptor cells. *Annu Rev Neurosci.* 2001;24:779-805.
10. Pepperberg DR, Birch DG, Hofmann KP, Hood DC. Recovery kinetics of human rod phototransduction inferred from the two-branched a-wave saturation function. *J Opt Soc Am.* 1996;13:586-600.
11. Pugh EN Jr, Lamb TD. Phototransduction in vertebrate rods and cones: molecular mechanisms of amplification, recovery and light adaptation. In: Stavenga DG, de Grip WJ, Pugh EN Jr, eds. *Molecular Mechanisms of Visual Transduction.* New York: Elsevier Science; 2000:183-255. *Handbook of Biological Physics.* Vol. 3.
12. Broekhuysen RM, Kuhlmann ED. Assay of s-antigen immunoreactivity in mammalian retinas in relation to age ocular dimension and retinal degeneration. *Jpn J Ophthalmol.* 1989;33:243-250.
13. Ho AK, Somers RL, Klein DC. Development and regulation of rhodopsin kinase in rat pineal retina. *J Neurochem.* 1986;46:1176-1179.
14. Stepanik PL, Lericous V, McGinnis JF. Developmental appearance, species and tissue specificity of mouse 23-kDa, a retinal calcium binding protein (recoverin). *Exp Eye Res.* 1993;57:189-197.
15. Johnson P, Williams R, Reese B. Developmental patterns of protein expression in photoreceptors implicate distinct environmental versus cell intrinsic mechanisms. *Vis Neurosci.* 2001;18:157-168.
16. Colombaioni L, Strettoi E. Appearance of cGMP-phosphodiesterase immunoreactivity parallels the morphological differentiation of photoreceptor outer segments in the rat retina. *Vis Neurosci.* 1993;10:395-402.
17. Fulton AB, Hansen RM. Recovery of the rod photoresponse in infant rats. *Vision Res.* 2003;43:3081-3085.
18. Birch DG, Hood DC, Nusinowitz S, Pepperberg DR. Abnormal activation and inactivation mechanisms of rod transduction in patients with autosomal dominant retinitis pigmentosa and the pro-23-his mutation. *Invest Ophthalmol Vis Sci.* 1995;36:1603-1614.
19. Lyubarsky AL, Pugh EN Jr. Recovery phase of the murine rod photoresponse reconstructed from electroretinographic recordings. *J Neurosci.* 1996;16:563-571.
20. Pepperberg DR, Birch DG, Hood DC. Photoresponse of human rods *in vivo* derived from paired flash electroretinograms. *Vis Neurosci.* 1997;14:73-82.
21. Pugh EN Jr. Vision: physical and retinal physiology. In: Atkinson RC, Hernstein RJ, Lindzay G, eds. *Stevens Handbook of Experimental Psychology.* New York: John Wiley & Sons; 1988.
22. Hansen RM, Fulton AB. Psychophysical estimates of ocular media density of human infants. *Vision Res.* 1989;29:687-690.
23. Werner JS. Development of scotopic sensitivity and the absorption spectrum of the human ocular media. *J Opt Soc Am.* 1982;72:247-258.
24. Larsen J. The sagittal growth of the eye. I. Ultrasonic measurement of the depth of the anterior chamber from birth to puberty. *Acta Ophthalmol.* 1971;49:239-262.
25. Hansen RM, Fulton AB, Harris SJ. Background adaptation in human infants. *Vision Res.* 1986;26:771-779.
26. Hansen RM, Fulton AB. Development of scotopic retinal sensitivity. In: Simons K, ed. *Early Visual Development, Normal and Abnormal.* New York: Oxford University Press; 1993:130-142.
27. Brown AM, Dobson V, Maier J. Visual acuity of human infants at scotopic, mesopic and photopic luminances. *Vision Res.* 1987;27:1845-1858.
28. Hood DC, Birch DG. Rod phototransduction in retinitis pigmentosa: estimation and interpretation of parameters derived from the rod a-wave. *Invest Ophthalmol Vis Sci.* 1994;35:2948-2961.
29. Breton ME, Schueller A, Lamb TD, Pugh EN Jr. Analysis of ERG a-wave amplification and kinetics in terms of the G-protein cascade of phototransduction. *Invest Ophthalmol Vis Sci.* 1994;35:295-309.
30. Schnapf JL, Nunn MJ, Meister M, Baylor DA. Visual transduction in cones of the monkey, *Macaca fascicularis.* *J Physiol (Lond).* 1990;427:681-713.
31. Wyszecki G, Stiles WS. *Color Science: Concepts and Methods, Quantitative Data and Formulae.* New York: John Wiley & Sons; 1982.
32. Pepperberg DP, Birch DG, Hood DC. Electroretinographic determination of human rod flash response *in vivo.* *Methods Enzymol.* 2000;316:202-223.
33. Friedburg C, Thomas MM, Lamb TD. Time course of the flash response of dark- and light-adapted human rod photoreceptors derived from the electroretinogram. *J Physiol.* 2001;534:217-242.
34. Smith NP, Lamb TD. The a-wave of the human electroretinogram recorded with a minimally invasive technique. *Vision Res.* 1997;37:2943-2952.
35. Cooper LL, Hansen RM, Darras BT, et al. Rod photoreceptor function in children with mitochondrial disorders. *Arch Ophthalmol.* 2002;120:1055-1062.